Nineteenth Australasian Wind Engineering Society Workshop, April 4-6, 2018, Torquay, Victoria

LES modelling of wind-flow around the Silsoe cube

R. H. Ong[1], J. Zhong[2], E. Eftekharian[3], Y. He[3], K.Kwok[1]

[1]*Center of Wind, Waves, and Water. School of Civil Engineering, The University of Sydney, NSW 2006, Australia.*
Email: robert.ong@sydney.edu.au, kenny.kwok@sydney.edu.au

[2]*School of Geography, Earth and Environmental Sciences, University of Birmingham, Birmingham, U.K.*
Email: j.zhong.1@bham.ac.uk

[3]*School of Computing, Engineering and Mathematics, Western Sydney University, NSW 2150, Australia.*
Email: e.eftekharian@westernsydney.edu.au, y.he@westernsydney.edu.au

ABSTRACT

The present study reports a preliminary investigation of the unsteady flows over the Silsoe 6 m cube with the wind perpendicular to one face using the Large-Eddy Simulation (LES) model. The computational work was carried out using the open-source toolbox OpenFOAM. The computed mean, standard deviation, maximum and minimum pressure coefficients of wind-flow simulation of Silsoe cube are shown to be in reasonable agreements with the full-scale observation and previously published CFD results.

1. Introduction

The correct and safe design of low-rise structures subjected to wind loads requires a realistic representation of the turbulent features found in the lower part of the atmospheric boundary layer in order to obtain accurate predictions of the structural response. Currently, standard design practice often involves the use of wind tunnel tests by taking into consideration the aerodynamics behaviour of the building and the expected site conditions in terms of terrain roughness and surrounding obstacles. However, numerical modelling such as Computational Fluid Dynamics (CFD) have been tested and proven to accurately predict wind flows around buildings and structures under conditions very close to the actual state (Tamura *et al.* 2008). The Silsoe 6 m cube (Richards *et al.* 2001; Richards and Hoxey 2012a, b; Richards and Norris 2015) provides a fundamental case study outlining the interactions between the wind and a structure. The form of the pressure coefficients follows Richards and Hoxey (2012a), given by:

$$C_{\bar{p}}(\bar{\theta}) = \frac{\bar{p}}{\bar{q}}, \qquad C_{\tilde{p}}(\bar{\theta}) = \frac{\sigma_p}{\sigma_q}, \quad C_{\hat{p}}(\bar{\theta}) = \frac{\hat{p}}{\hat{q}}, \qquad C_{\check{p}}(\bar{\theta}) = \frac{\check{p}}{\hat{q}} \tag{1}$$

where p is the surface pressure and q is the reference dynamic pressures measured at cube height (6 m) in the approach flow. σ_p is the standard deviation of pressure, while $\bar{p}$, $\hat{p}$, $\check{p}$ are the mean, maximum and minimum values of pressure respectively.

2. Numerical modelling

The simulations were performed using the open-source Computational Fluid Dynamics (CFD) toolbox, OpenFOAM. The flow simulations for both the precursor and the flow around bluff body were conducted using the Large Eddy simulation (LES) sheme, which limit the computational cost by only computing the large scales structures while the effect of the smallest scales are modelled. To separate the large resolved scales from the small unresolved scales (termed subgrid-scales, SGS), a filtering operation with a defined cutoff length (Δ) is necessary. Its characteristic scale is usually taken to be the power average of grid sizes in all directions, given by:

$$\Delta = \left(\delta_x \delta_y \delta_z\right)^{\frac{1}{3}} \tag{2}$$

Here we implemented a LES model called k-equation-eddy model, that uses the eddy viscosity approximation. The SGS eddy viscosity ν_{SGS} is defined as

$$\nu_{\mathrm{SGS}} = C_k \sqrt{\frac{k_{SGS}}{\Delta}} \tag{3}$$

The SGS kinetic energy (k_{SGS}) is solved by the transport equation, and the model constants of C_k and C_e have default values of 0.094 and 1.048, respectively.

The inlet boundary condition of atmospheric boundary layer was generated using a precursor domain in a 720 m x 60 m x 40 m (*L* x *W* x *H*) empty domain. A periodic boundary condition is imposed in both streamwise and spanwise directions, with the flow are driven by a pressure gradient. The top domain had a symmetry boundary condition applied. The velocity was prescribed at the upstream boundary, with a mean velocity of 6 m/s at the height of 6 m, and a prescribed pressure outlet boundary condition was set at the downstream boundary. Table 1 is a summary of the parameters in the ABL simulation. Once both the mean profile and the temporal and spatial fluctuations of the flow has reached a statistical behavior of quasi-steady, the data of a cross-sectional plane is sampled and stored to be used to provide inflow boundary conditions for the main simulation domain (successor domain). The flow was sampled at 0.05 s intervals for a period of 25 min, which was broken into two 12.5 min blocks of data. The flow was allowed to settle for the first 30 s of each run, and then 12 min data was recorded. The successor domain was modeled using the standard Smagorinsky model (Smagorinsky, 1963) with C_s=0.18 damped at the wall with a rough wall function based on velocity, using Spalding's law to give a continuous turbulent viscosity at the wall. The successor domain is 90 m long, 60 m wide, and 40 m high using a 90 x 120 x 160 mesh with a uniform grid across the domain height (Fig. 1).

Table 1. ABL simulation specification

Parameter	Value
Domain height [m]	H = 40
Reference velocity [m/s]	u_{ref} = 7.78
Roughness [m]	z_0= 0.001
von Karman constant [-]	κ = 0.41
kinematic viscosity of air [m^2/s]	ν = 1.455 x 10^{-5}
friction velocity [m/s]	u_*= 0.384

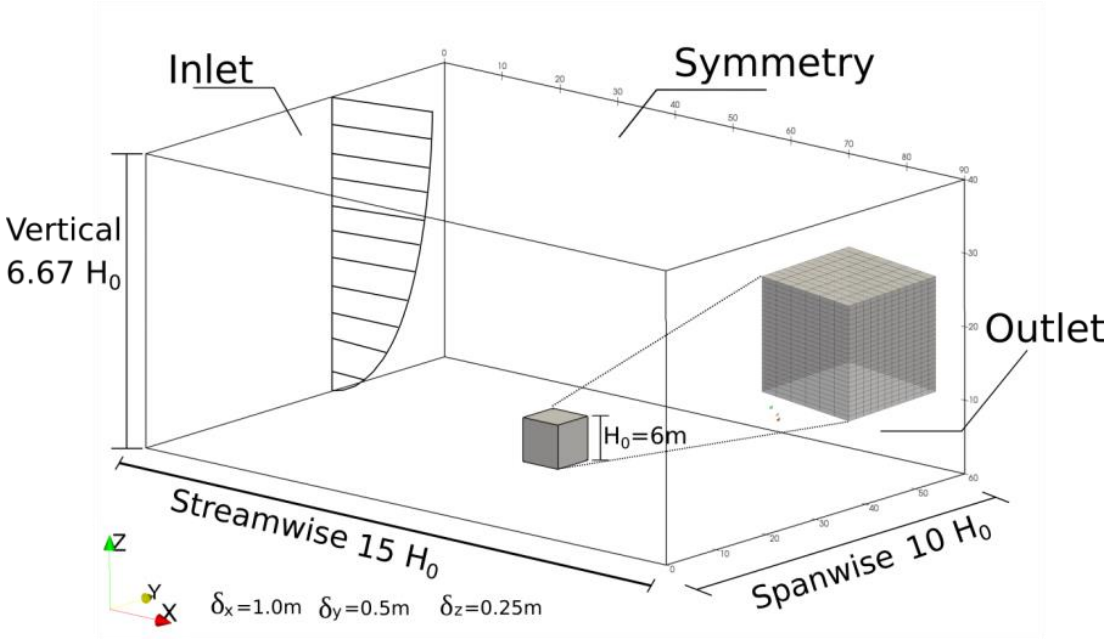

Fig. 1. Schematic of the successor domain with the precursor ABL prescribed at the inlet.

3. Results and discussions

3.1. Flow fields: mean profile and velocity variances

The target logarithmic profile is plotted in dashed line, and the overall profile varies by about 5-10%. The log-layer near the ground shows reasonable agreement. The top profile slightly deviates from the log-law, however, since the top part is not as important as the near-wall region, the mismatch at the top is seldom observed. Velocity variance is a measure the turbulence fluctuations within the atmospheric boundary layer, which was normalized by u_*^2.

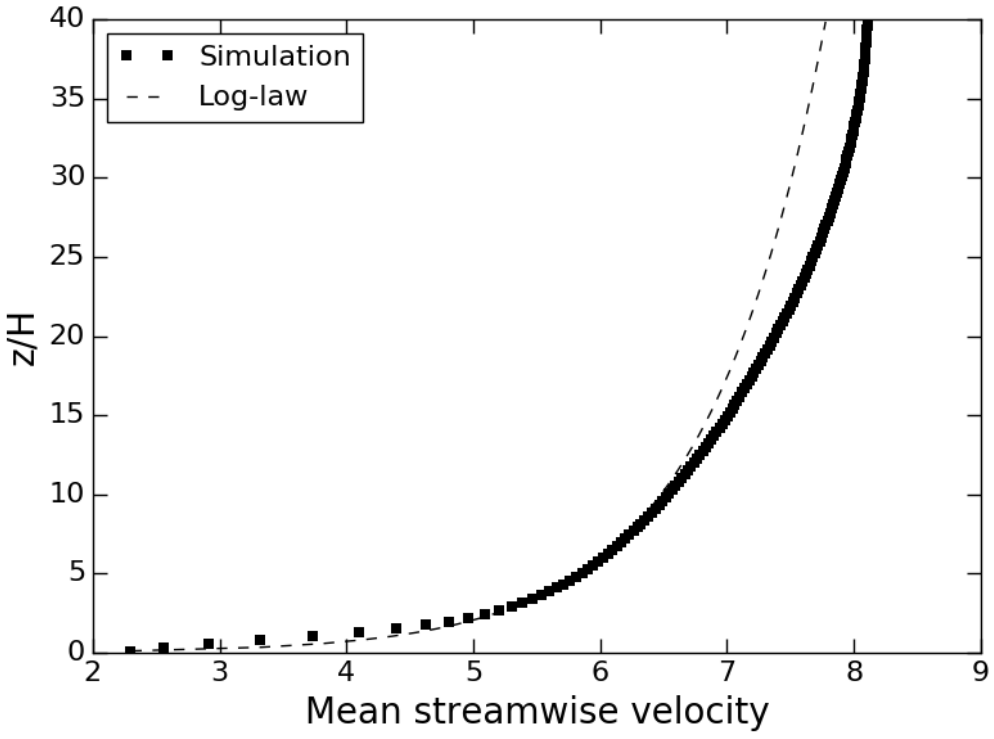

Fig. 3. Vertical profiles of the mean streamwise velocity.

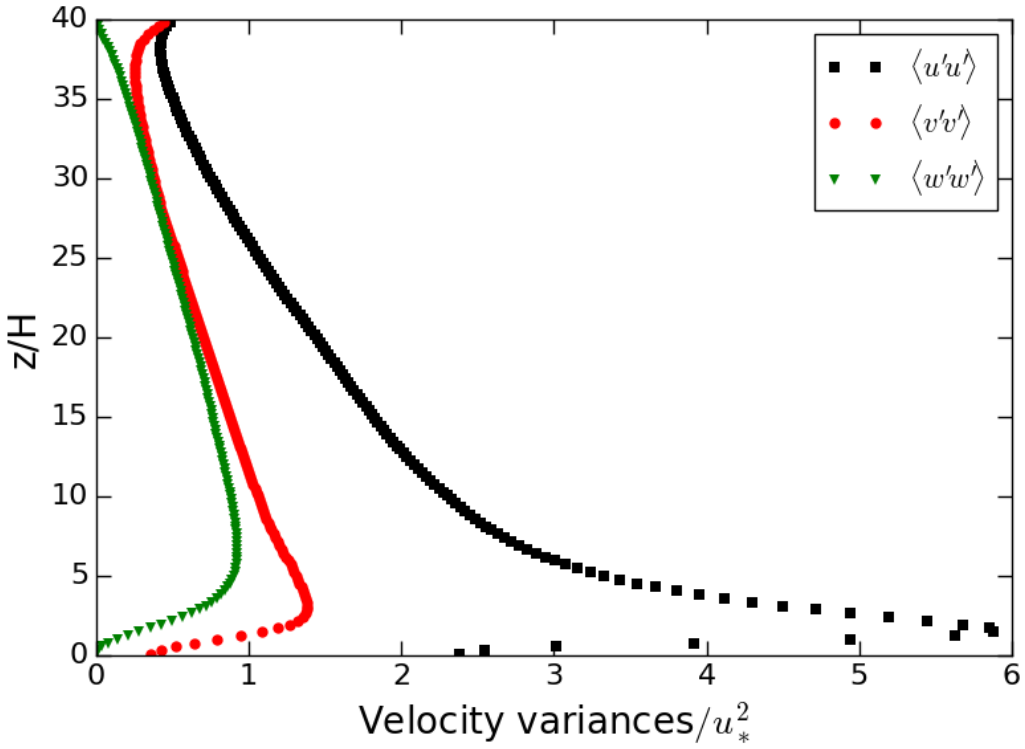

Fig. 4: Vertical profiles of the normalized variance of the velocity.

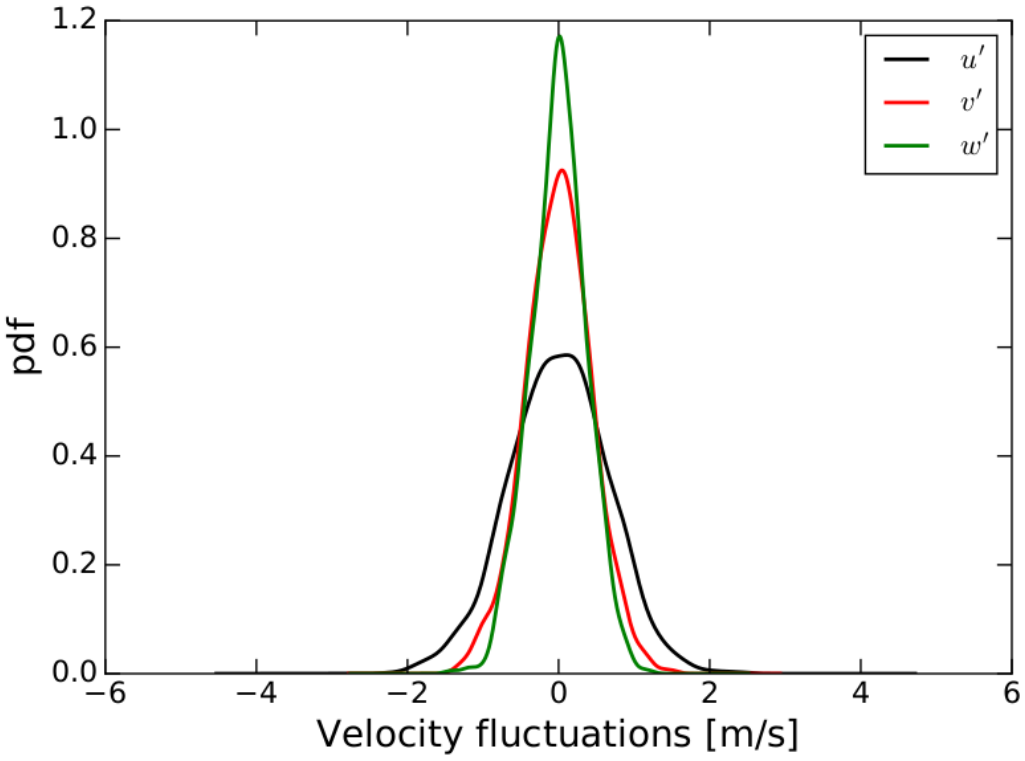

Fig. 5: Probability density function at 6m height.

The *u* component displays strong fluctuations with large troughs and relatively low peaks, which is clearly reflected in the PDF of the fluctuations *u'*, whereas the fluctuation *v'* and *w'* follows approximately the Gaussian distributions.

3.2. Silsoe pressure coefficients of wind-only for a wind direction of 90^0

The computed pressure coefficients with the wind perpendicular to one face for the horizontal (Fig. 4) and vertical (Fig. 5) cross-sectional rings for are validated against both the full-scale measurements and from Richards and Norris (2015) LES data.

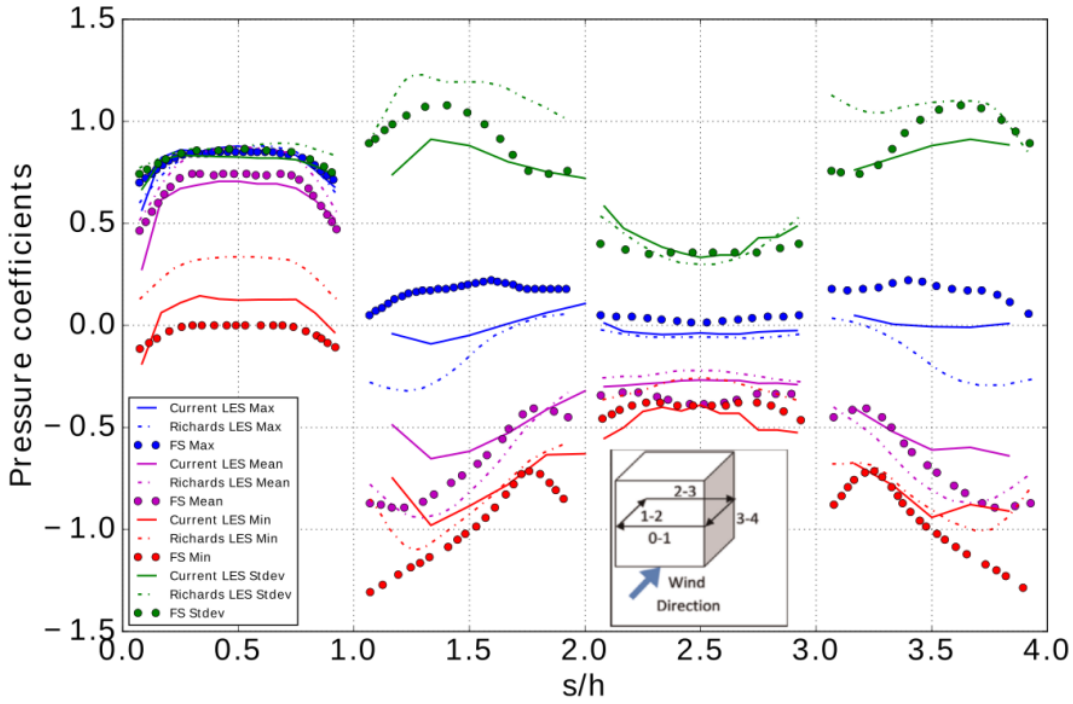

Fig. 5. Cp_s of a horizontal ring under the wind direction of 90^0.

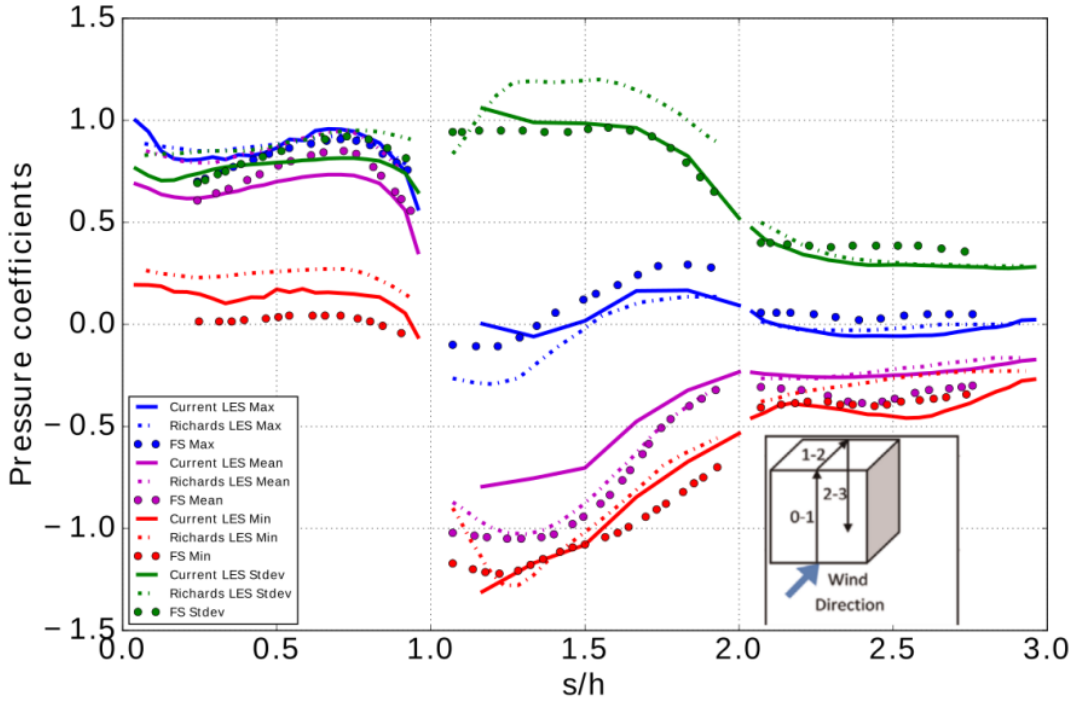

Fig. 5. Cp_s of a vertical ring under the wind direction of 90^0.

The current mean *Cp* values of windward face (vertical ring lines 0-1 and 1-2) showing some deviations from the FS and LES data, which may be partly due to the relatively coarse grid used here. Moreover, implementing other numerical schemes with low dissipative behavior and numerical stability may improve the overall agreement with FS data.

4. Conclusions

We presented a wall-modelled LES study of turbulent boundary layer flow using a precursor method to produce realistic flow statistics. Periodic boundary conditions were applied in the streamwise and spanwise directions while symmetry boundary condition was imposed at the top. We validated the prediction of wind loading of low-rise building using Silsoe cube. The evaluation of CFD results for wind loads under neutral ABL show reasonable agreement with the published data.

References

Tamura, T., Nozawa, K., Kondo, K., 2008. AIJ guide for numerical prediction of wind loads on buildings. Journal of Wind Engineering and Industrial Aerodynamics, 96, 1974-1984.

Richards, P.J., Hoxey, R.P., Short, L.J., 2001. Wind pressures on a 6 m cube. J. Wind Eng. Ind. Aerodyn. 89 (14–15), 1553–1564

Richards, P.J., Hoxey, R.P., 2012a. Pressures on a cubic building—Part 1: full-scale results. J. Wind Eng. Ind. Aerodyn. 102, 72–86.

Richards, P.J., Hoxey, R.P., 2012b. Pressures on a cubic building—Part 2: quasi-steady and other processes. J. Wind Eng. Ind. Aerodyn. 102, 87–96.

Richards, P.J., Norris, S., 2015. LES modeling of unsteady flow around the Silsoe cube. J. Wind Eng. Ind. Aerodyn. 144, 70-78.

Smagorinsky, J., 1963. General circulation experiments with the primitive equations. Mon. Weather Rev. 91, 99-164.